Numerical Study of Fin Effects on Thermal Performance of Annular Solar Salt-Layered Vacuum Collector Tubes

Wang, Hua[a], Li, Xuyang[a], Xie, Shukuan[b,a], Zhang, Lin[a]*

a. School of Mechanical and Power Engineering, Henan Polytechnic University, 2001 Century Avenue, Jiaozuo 454003, Henan, P R China

b. No.1 Songshan South Road, Zhengzhou City, Henan Province, PR China

Previous research showed that integrating phase change materials with solar tubes stabilizes heat transfer fluid temperature, but the low conductivity of phase change materials limits solar tube performance. Although studies on fluid properties and heat transfer behavior are extensive, the critical influences of fin shapes' effect are limited. This paper introduces an innovative design: an all-glass vacuum tube with a solar salt sleeve surrounded by outer fins. Numerical simulations compare heat transfer dynamics of straight rectangular, circular, and trapezoidal fins. The study examines how these shapes affect temperature field evolution and phase transition. Results indicate: 1) Fins reduce temperature disparity between solar salt and heat transfer fluid, with rectangular fins showing the greatest improvement of only 12°C. 2) Fins accelerate salt phase transition, albeit with a slight delay in initiation. Adding trapezoidal ring fins reduces the complete phase change duration by 5 minutes. 3) the tube with 4 rectangular fins demonstrates the highest temperature field and maximum total heat storage of 269kJ, highlighting its superiority.

Key words: *solar vacuum collector tube; phase change materials; fins; thermal characteristics*

1. Introduction

Applying solar vacuum collector to Compound Parabolic Concentrator (CPC) can obtain a heat source higher than 100°C [1]. It can be used in heating, absorption cooling, drying, and even power generation. However, due to the disadvantages of unstable and discontinuous of solar energy [2], unlike the salt gradient solar pond [3,4], solar still [5,6], buildings energy conservation [7], the instantaneous fluctuations in solar radiation frequently exert a significant impact on the heating temperature of the Heat Transfer Fluids (HTF) within the CPC's solar vacuum collector.

Thermal energy storage materials, particularly phase change materials (PCMs), provide crucial support for overcoming solar energy's inherent discontinuity and instability while enhancing system performance [7-9]. Given the global prevalence of climate change and water scarcity, PCMs applications have gained heightened significance in solar-thermal integration [10]. Analysis of technology readiness levels and levelized storage costs confirms PCMs' suitability for large-scale solar thermal applications [7]. As one of the most extensively studied thermal storage media, PCMs have been systematically evaluated through innovative testing methodologies. Huang et al. [11] developed a solar-thermal test platform employing controllable heaters to simulate varying solar inputs.

Despite their tunable transition temperature capabilities, the applications of PCMs are constrained by their low thermal conductivity behavior [12]. The incorporation of nanoparticles, with their exceptional thermal conductivities and low heat capacities, into PCMs is one of the most frequently employed procedures nowadays [13], many reports indicated substantial improvements in heat transfer when employing these fluids [14]. D Wen et al. [15] found that carbon nanotube nanofluids become destabilized at temperatures exceeding 60-70°C due to the failure of the dispersant. In the context of enhancing heat transfer in PCMs applied in CPC, the development of more stable and reliable methods is necessary.

Many researches have been focused on the application of PCMs in solar thermal utilization, while limited attention has been given to the novel configuration of PCMs encapsulation as a cladding layer for CPC. Particularly, systematic investigations into the impact of fin configurations on heat transfer enhancement within the PCMs layer remain notably scarce in existing literature. The authors of this study have previously examined the impact of incorporating PCMs on the thermal characteristics of straight-through solar vacuum collector tubes [4]. Using solar salt as PCMs, the influence of the thermodynamic properties of the straight-through solar vacuum collector tube was investigated both experimentally and numerically. The results indicate that, after 4-hour cooling, the temperature within the solar collector tube with PCMs was notably higher than that without PCMs. It was also observed that the low thermal conductivity of the PCMs diminished its positive contribution to the thermal performance of the novel tubes. The inclusion of phase change materials will affect the radial distribution of the temperature field within the straight-through solar vacuum collector tube, owing to the poor thermal conductivity of molten salt [16, 17]. To improve the thermal conductivity of phase change materials, there are generally two ways. Apart from adding materials with superior heat transfer capabilities to PCMs [19], another strategy involves enhancing heat transfer by optimizing the heat exchanger structure [20]. V. K. [21] found that the absorber plate with polygonal fins tested with phase change material yields a higher temperature. To improve the low heat transfer coefficient between heat exchangers and seawater, Yao et al. [22] proposed a new type of heat exchanger structure with external fin turbulators. The second method is primarily employed in this study.

Despite extensive studies conducted on fluid properties and heat transfer behavior, there remains a notable lack of research specifically focusing on the influence of fin shapes on heat transfer for solar collector tubes. Based on preliminary research, this study establishes a numerical model of the straight-through solar vacuum collector tube with different fin configurations. The influence of incorporating fins with varying shapes, quantities, thicknesses, and heights on the thermal characteristics of the collector tube has been investigated. The findings of this study establish a theoretical foundation for the design optimization of solar collector tubes integrated with high-temperature molten salt layer. Practical implementation of these research outcomes in evacuated collector tubes is expected to significantly enhance the thermal output stability of the solar thermal applications.

2 Numerical model

2.1 Geometrical model and physical fields

The straight-through solar vacuum collector tube with annular salt layer consists of a high borosilicate transparent glass outer tube, a vacuum layer, a tube with a selective coating surface, a solar salt PCMs layer, a stainless-steel inner tube, and a HTF from the outside to the inside. As shown in fig. 1, the fins are added to the outer surface of the stainless-steel tube. This study simplified the vacuum layer part as in the previous study [4]. The heat loss caused by the vacuum tube is applied to the outer surface of the selective absorption coated tube in the form of a loss coefficient. The selective absorption coating tube, heat exchange tube with external fins is constructed in the numerical geometry model.

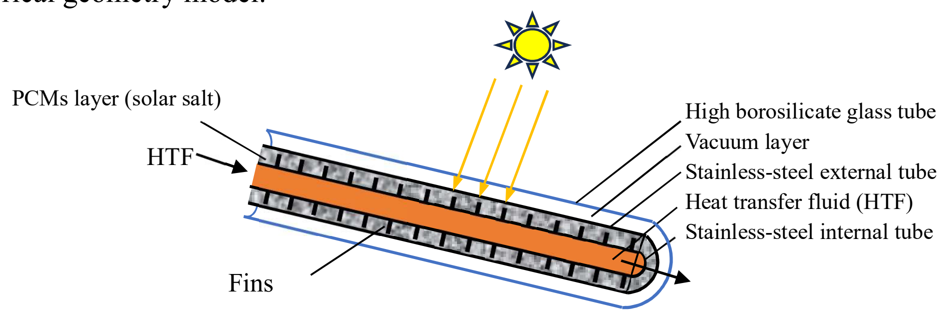

(a) The straight-through solar vacuum collector tube with annular solar salt layer

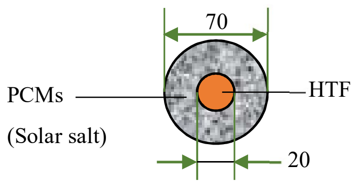

(b) cross-section of the optical tube

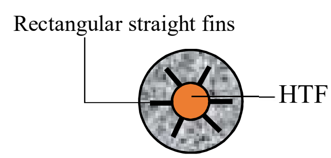

(c) cross-section of tube with rectangle straight fins

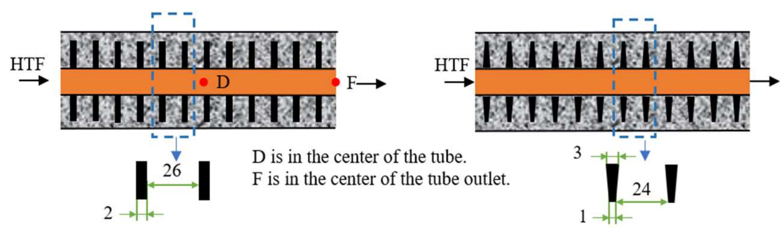

(d) axial section of tube with ring fins

(e) axial section of tube with trapezoid fins

Fig. 1 Section structures of the tubes involved in this study (unit: mm)

In order to facilitate the comparison with the straight-through solar vacuum collector tube without added fins, in the geometric model, the heat exchange tube is stainless steel with 20 mm diameter, the selective absorption coating tube is glass with 70mm diameter, and the tube length is 630 mm. As shown in fig. 1, a geometric model of a straight-through solar vacuum collector tube with rectangular straight fins, circular ring fins and trapezoidal ring fins had been established to explore the optimal fin shape. The height of the fins, the thickness and the total surface area of the fins are equal, and the fins are made of stainless steel. The specific parameters are shown in tab. 1.

Tabel 1 The fin parameters of various shapes

Cases	Shapes of Fins	Thickness /mm	Height /mm	Surface area of each fin /m^2	Description
Case A	—	—	—	—	Without any PCMs
Case B	Rectangular straight fins	2	20	0.0126	Length 630 mm
Case C	Round ring fins	2	20	0.002512	D_i=20 mm, D_e=40 mm
Case D	Trapezoid ring fins	Upper 1 Bottom 3	20	0.002515	Isosceles trapezoidal unit fins rotated 360° around the x-axis and arranged at equal spacing

The physical fields incorporated in this study using the COMSOL Multiphysics software encompass fluid heat transfer, phase transition heat transfer, and turbulent flow. Fluid heat transfer is employed to simulate heat transfer, convection, and radiation within fluids. Both the fluid domain and the phase transition heat transfer domain are integral parts of this model. The phase transition heat transfer field is utilized to simulate the energy transfer of phase transition materials within the phase transition region. Within the physical field of this model, two standard equations have been adopted: the κ-ε model interface, which couples the heat transfer equation with the turbulence equation. The numerical model employed in this study is based on the our previously established model in reference [4], which has been validated by experimental results.

2.2 Initial and boundary conditions

The initial conditions for the temperature field were set to the room temperature of the study subject, and the initial flow rate of the fluid was zero. The vacuum tube has been simplified, consisting only of the selective absorption coating tube and the heat exchange tube. However, in the selective absorption coating tube, due to the minimal light transmittance loss of the vacuum layer, only effective solar radiation was applied to the outer surface. Additionally, for heat loss considerations, the boundary conditions of the selective absorption coating are as shown in eq. (1).

$$q_{\mathrm{act}} = q_{\mathrm{s}} - q_{\mathrm{loss}} \tag{1}$$

where q_{act} is the solar radiation power actually absorbed and converted by the selective absorption coating tube, W/m^2; q_{s} is the effective solar radiation power received by the selective absorption coating tube, W/m^2; q_{loss} is the solar radiation power loss on the outer surface of the selective absorption coating tube, W/m^2, calculated by eq. (2),

$$q_{\mathrm{loss}} = u_{\mathrm{loss}} \times (T_{\mathrm{i}} - T_{\mathrm{a}}) \tag{2}$$

where u_{loss} is the total heat loss coefficient, W/(m^2•°C), obtained from eq. (3) [23]; T_{i} is the surface temperature of the selective absorption coating tube, and Ta represents the ambient temperature, °C.

$$u_{\mathrm{loss}} = \left(\frac{1}{h_{\mathrm{i}}} + \frac{1}{h_{\mathrm{o-c}} + h_{\mathrm{o-r}}} \right)^{-1} \tag{3}$$

where h_{i} is the radiation heat transfer coefficient between the selective absorption coating tube and the vacuum tube, W/(m^2•°C), calculated by eq. (4) [23]; $h_{\mathrm{o\text{-}c}}$ is the radiation heat transfer coefficient between the vacuum tube and the sky, W/(m^2•°C), calculated by eq. (5) [23]

$$h_{\mathrm{i}} = \sigma\left(T + T_{\mathrm{a}}^{2}\right) \times \left(T_{\mathrm{i}} + T_{\mathrm{a}}\right) \Big/ \left[\frac{1}{\varepsilon_{\mathrm{O}}} + \frac{\mathrm{A_o}}{\mathrm{A_i}} \left(\frac{1}{\varepsilon_{\mathrm{i}}} - 1 \right) \right] \tag{4}$$

where σ is the Stefan-Boltzmann constant, σ =5.6710^{-8}W / (m^2• K^4); ε_{o} and ε_{i} are the emittance on the surface of vacuum tube and selective absorption coating tube, respectively; $\mathrm{A_o}$ and $\mathrm{A_i}$ are the surface area of vacuum tube and selective absorption coating tube, m^2 respectively,

$$h_{\mathrm{o\text{-}c}} = 5.7 + 3.8 \times v_{\mathrm{wind}} \tag{5}$$

where v_{wind} is wind speed, m/s; the experiment in this study is conducted in room, so it is be ignored, and $h_{\mathrm{o\text{-}c}}$=5.7 W/(m^2•°C). $h_{\mathrm{o\text{-}r}}$ in eq. (3) is the radiant heat transfer coefficient between evacuated pipe and sky, it can be written as [23],

$$h_{\mathrm{o-r}} = \sigma\left(T_{\mathrm{s}}^{2} + T_{\mathrm{a}}^{2}\right) \times \left(T_{\mathrm{s}} + T_{\mathrm{a}}\right) \Big/ \left(\frac{1}{\varepsilon_{\mathrm{o}}} \right) \tag{6}$$

where T_{s} is the atmosphere temperature, and calculated by the following equation [23]:

$$T_s = 0.0522\ T_a^{1.5} \tag{7}$$

3 Effect of the fin plate shape on the thermal characteristics of the collector tube

Our previous study [4] demonstrates that adding a PCMs layer primarily influences the uniformity of the radial distribution of the collector's temperature field, whereas the flow rate of the HTF mainly affects the uniformity of the axial distribution of the collector's temperature field. Therefore, the HTF velocity is ignored in the study of the fin shape. Furthermore, the study found that, in the case of 1 hour of solar radiation, if the material is intended to undergo a complete phase transition, the solar radiation power must be at least 200 W/m^2 . Consequently, the solar radiation power is set to 300 W/m^2 in this study.

3.1 Effect of the fin shape on the radial distribution of the collector tube temperature field

Fig. 2 presents radial temperature distribution at the axial middle section of the collector tubes at different times for the four cases. It can be observed that all cases maintain the inherent radial temperature gradient of decreasing from outer to inner. As shown in fig.2, significant phase change was observed at the 45th minute for the melting point of the molten salt employed in this study is approximately 222°C [4]. Notably, case B (rectangular straight fins) displays reduced stratification at 15–45 minutes but develops localized high-temperature zones (60 minutes) between fins. This phenomenon arises from the axial flow of fully liquefied PCMs within fin-created enclosures, where diminished thermal resistance promotes heat accumulation. Thermal performance comparisons reveal: case D achieves the highest temperature of 314°C, marginally exceeding the blank condition of case A by 1°C, yet reduces thermal gradient to 15°C (vs. 67°C in case A), accounting for the heat transfer enhancement of the fins. Case C attains a peak temperature of 306°C with an 18°C thermal gradient. Case B demonstrates optimal temperature uniformity (12°C gradient) but the lowest peak temperature of 296°C.

To clarify the influence of fin shapes on the radial temperature distribution within the collector tube, we have calculated the average temperature of the outer surface of the selective absorption coating tube. Additionally, as shown in fig. 3, the temperature differences between this temperature and the center point of the collector tube (point D) for all the cases have been computed. It is evident that the incorporation of fins reduces the radial temperature difference within the collector tube. The collector tube with rectangular straight fins (case B) exhibited the minimal radial temperature differential, followed by case D with trapezoidal ring fins, while the circular annular fins (case C) showed the largest gradient. At the 60th minute mark post full melting, case C displayed a temperature differential of 18°C, exceeding case B and case D by 6°C and 3°C, respectively. Specifically, during solar radiation heating, the rectangular straight fin collector tube exhibits the smallest radial temperature difference, followed by the trapezoidal fin tube, and the ring fin tube shows the largest difference.

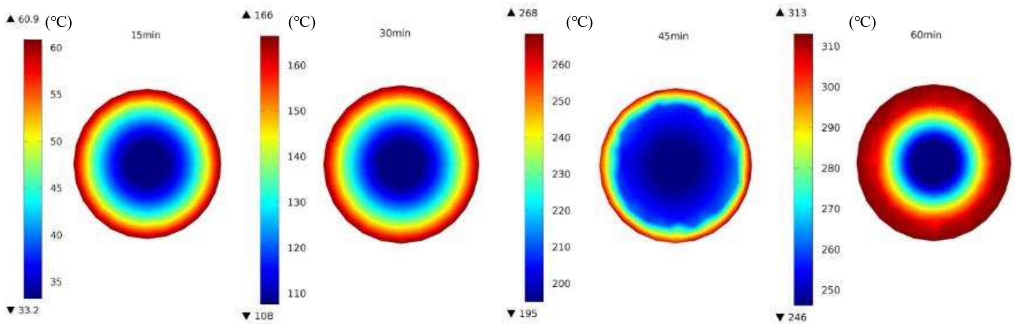

(a) Case A: Radial distribution of collector tube temperature without fins

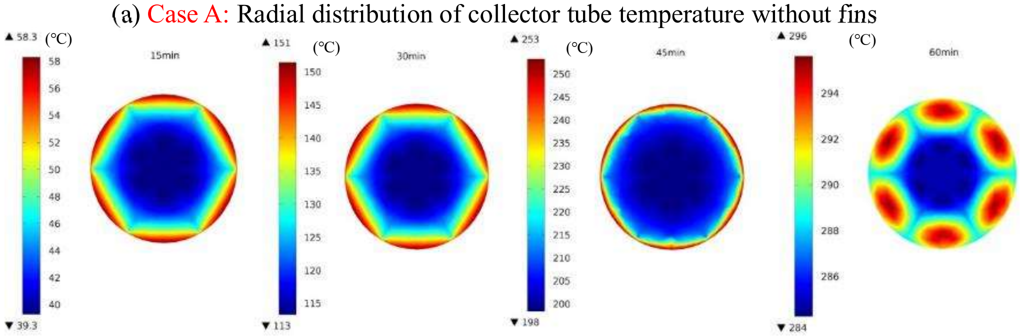

(b) Case B: The radial distribution of the collector tube with rectangular

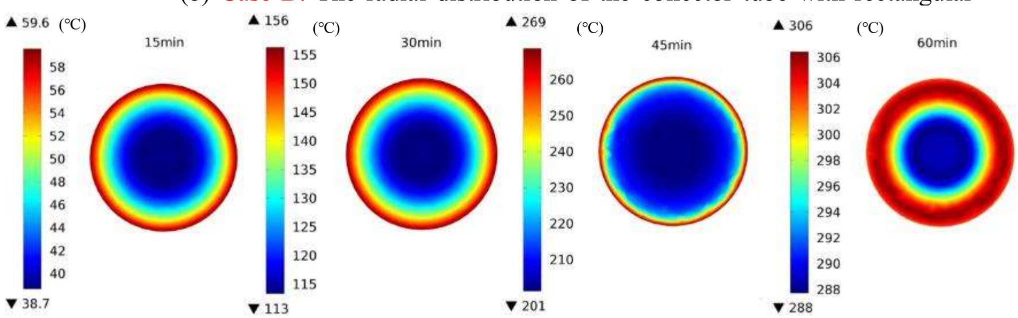

(c) Case C: Radial distribution of collector tube with circular ring fins

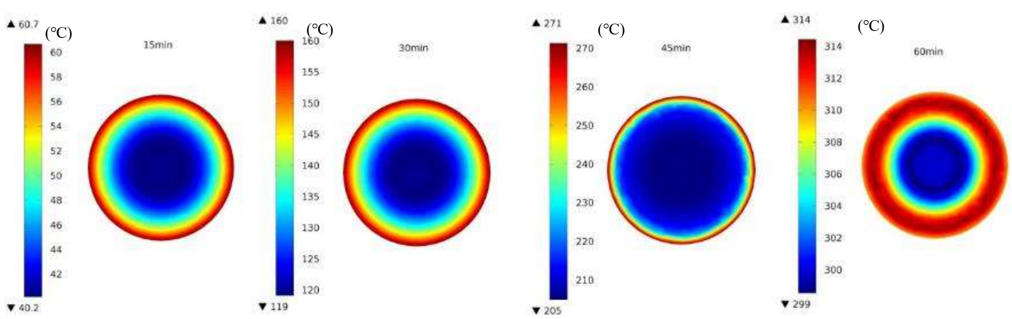

(d) Case D: Radial distribution of collector tube with trapezoidal ring

Fig. 2 The radial temperature distribution of solar collector tubes without fins and with different fins under different times

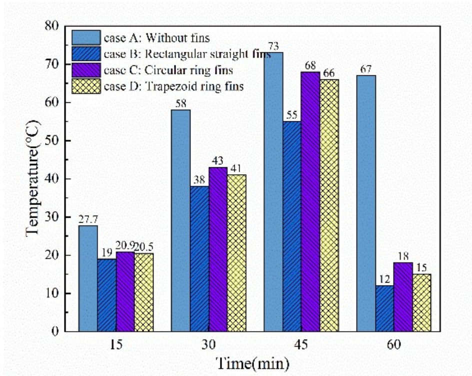

Fig. 3 The radial average temperature-difference of the solar collector tubes with different shapes fins at different times

It can also be observed in fig. 3 that the radial temperature difference of the collector tube gradually increases within the first 45 minutes and then decreases again thereafter. This is due to the fact that during the first 45 minutes, the phase change material is primarily in the solid state, and the radial heat transfer mode is mainly thermal conduction. As the heating time increases, the phase change material undergoes a complete phase change, shifting the dominant mode of heat transfer to convection. Consequently, the heat transfer coefficient becomes larger, and the heat transfer speed accelerates, causing the radial temperature difference to begin decreasing. A comprehensive analysis of fig. 2 and fig. 3 reveals that under continuous solar radiation, the incorporation of rectangular straight fins results in better uniformity of the radial distribution and superior radial heat transfer performance compared to trapezoidal ring fins and circular ring fins.

3.2 Shape of fins effect on the axial temperature distribution of the collector tubes

Previous research has found that phase change materials do not disrupt the uniformity of the axial distribution of the collector tube temperature [4]. In this section, we have investigated the impact of various fin shapes on the axial distribution of the collector temperature. The primary objective is to identify the optimal fin shape that has minimal influence on the axial distribution uniformity of the collector tube temperature. Fig. 4 displays the axial temperature distribution of the collector tube without fins and with fins of three different shapes at 60 minutes.

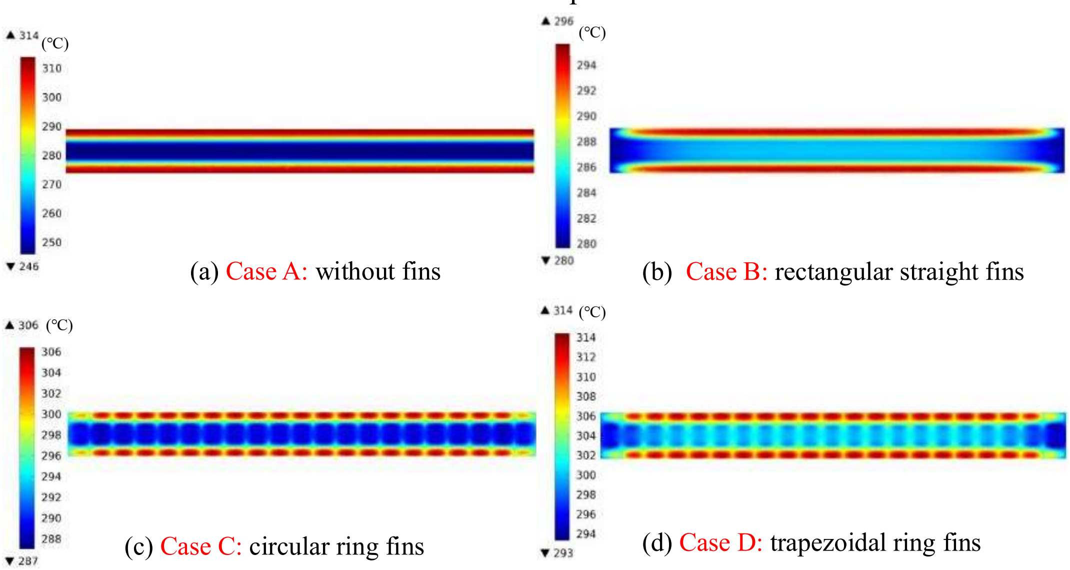

(a) Case A: without fins

(b) Case B: rectangular straight fins

(c) Case C: circular ring fins

(d) Case D: trapezoidal ring fins

Fig. 4 The axial temperature field distribution of solar collector tube without/with fin in the 60th minute

As evident from the fig.4, the addition of fins disrupts the uniformity of the axial temperature distribution within the collector tube. Among the three fin shapes, rectangular straight fins have the least impact on the uniformity of the axial temperature distribution. In contrast, both circular ring fins and trapezoidal ring fins create high-temperature agglomerations in the spaces between two fins, leading to a division phenomenon in the axial direction, and the uniformity of the axial temperature distribution within the collector tube has been compromised. Consequently, the temperature distribution of the collector tube becomes non-uniform in the axial direction.

In order to comprehensively evaluate the influence of fin shapes on the uniformity of axial temperature distribution within the collector tube during the entire solar radiation process, the temperature changes at the middle point (D) and the outlet center point (F) have been monitored. The temperature of these two points was recorded at each moment during the heating process, and the temperature difference was calculated. Fig. 5 shows the temperature difference between these two points. It can be observed that after 45 minutes, the temperature of the heat transfer fluid (HTF) in the finned cases significantly increased following phase change completion, whereas case A (without fins) showed no notable variation. As previously mentioned, from the 45th minute, the PCMs was undergoing phase transition, absorbing substantial heat with minimal temperature change. During this stage, the PCMs acted as a constant-temperature heat source for the HTF. Between 45 and 60 minutes, the constant high temperature heat source heated HTF rapidly, and the prolonged heat exchange duration caused the temperature at point F to surpass that at point D. Regarding the temperature rise of the HTF outlet (Point F) compared to the collector tube center (Point D), the circular fins achieved a maximum temperature increase of 18.6°C, followed by trapezoidal fins (10.0°C) and rectangular straight fins (9.1°C). These results demonstrate that adding fins not only enhances heat transfer but also significantly improves the thermal performance of the HTF.

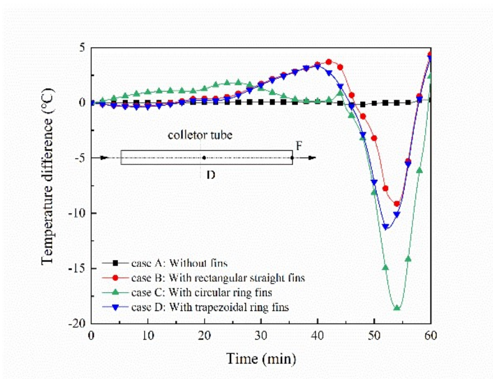

Fig. 5 The graph changing temperature-difference between points D and F (T_D-T_F) in solar collector tube with time

3.3 Influence of the shape of fins on the phase change process of PCMs

Fig. 6 shows the average liquid rate variation of the PCMs in collector tubes without and with the three types of fins. As shown in fig. 6, liquefaction in the collector tube without fins occurs earliest, while in the tube with rectangular straight fins occurs the latest. This is due to the low thermal conductivity of PCMs, and in the absence of fins, it is more prone to the radical heat agglomeration of PCMs, resulting in localized phase transition. However, contrary to the initial liquefaction trend, the PCMs in the tube without fins completes its phase change at the 58th minute which is the latest one. Case D with trapezoidal ring fins achieves complete phase change first using 52.5 minutes, followed by cases B and C of about 55 minutes. This is because once phase change occurs, the fins can rapidly transfer heat to other materials that have not yet changed, allowing the PCMs to undergo phase change more uniformly.

Fig. 7 compares the liquid fraction distribution of the internal phase change material between those with trapezoidal ring fins and rectangular straight fins at different times. As can be seen, the phase transition process occurs from the outside to the inside along the radial direction. The phase change material in the collector tube

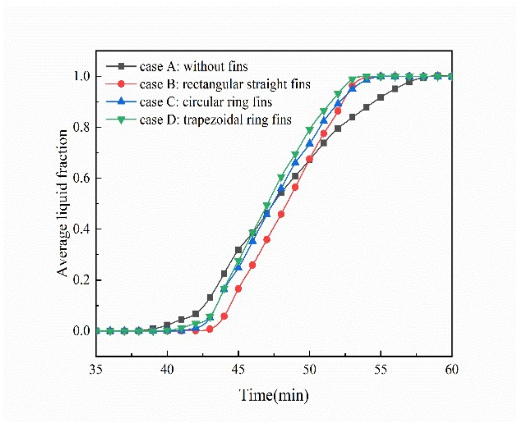

Fig. 6 The average liquid fraction of the PCMs in the solar collector tube without adding fins and adding three-shaped fins

with trapezoidal ring fins first undergoes a change near the boundary of the fins, and subsequently, the material within the spacing between the two fins initiates the phase transition. The phase transition process is not uniform across the axial.

In contrast, the axial distribution in the collector tube with rectangular straight fins is uniform. A comprehensive analysis of fig. 6 and fig. 7 reveals that the addition of fins delays the onset of the phase transition in the collector tube. Among the three types of fins, trapezoidal ring fins have the least impact on the starting time of the phase transition, resulting in the earliest onset. The axial distribution of the phase transition material in the heat collection tube with rectangular straight fins is the most uniform; however, the starting time of the phase transition is the latest.

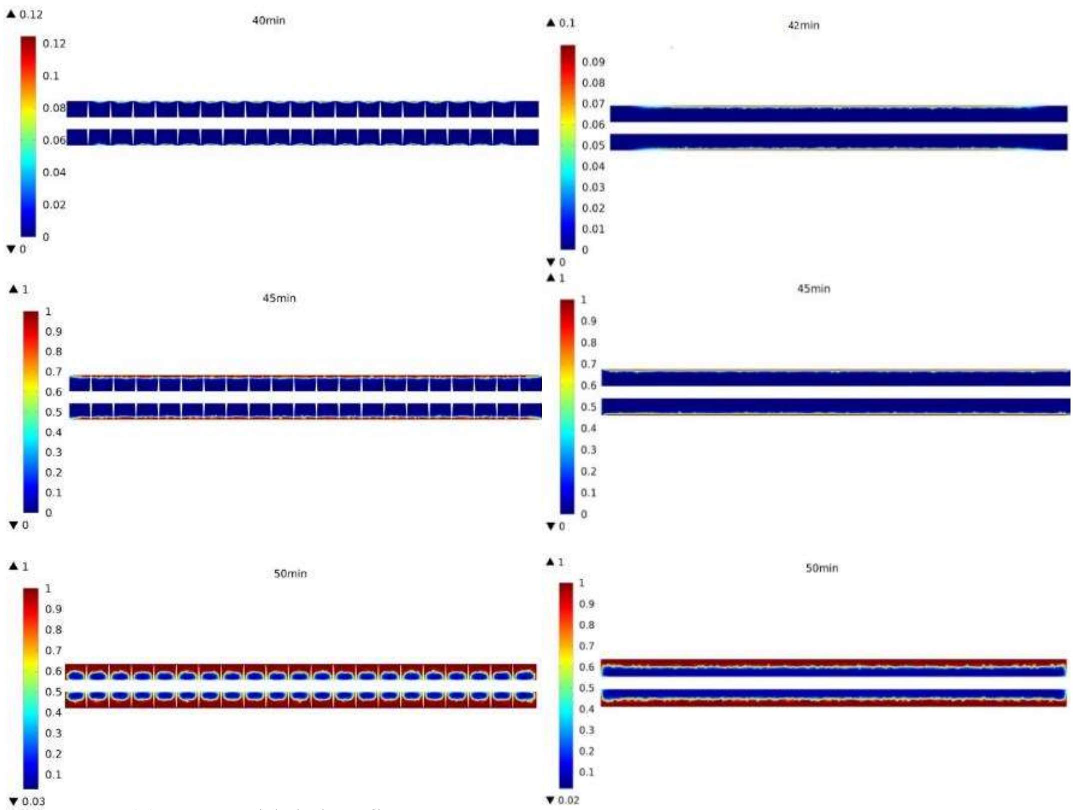

(a) trapezoidal ring fins (b) rectangular straight fins

Fig. 7 The liquid fraction distribution of the internal PCMs in the solar collector tube adding trapezoidal ring fins and rectangular straight fins at different times

4. The effect of the number of the fins on the thermal characteristics of the collector tube

From the above study, it is evident that rectangular straight fins outperform circular ring and trapezoidal ring fins in terms of the uniformity and heat transfer performance of the radial temperature distribution within the collector tube. Rectangular straight fins also have the least adverse effect on the axial temperature distribution uniformity of the collector tube. In this section, we have selected rectangular straight fins to investigate the impact of the number of the fins on the temperature distribution and heat storage performance of the collector tubes. While examining the impact of the number of fins, a constant fin height of 20 mm and fin thickness of 2 mm are considered. In terms of disrupting the uniformity of temperature, 2, 4, 6, and 8 fins were evenly distributed on the pipe wall. Details are shown in tab. 2.

After the addition of the fins, the total heat storage of the collector tube mainly consists of two parts: one comes from the phase change material, including sensible heat and latent heat; the other comes from the sensible heat storage of the fins. The sensible heat storage Q_s is calculated by eq. (8), and the latent heat storage Q_L of phase change is calculated by eq. (9),

$$Q_s = cm(T_{t1} - T_{t2}) \tag{8}$$

where c is the specific heat capacity of the material, kJ / (kg•°C); m is the mass of the material, kg; T_{t1} and T_{t2} are the temperature of the material at time t_1 and t_2 respectively, the temperature of the material is the average temperature of the material.

$$Q_L = m_{PCMS} L \tag{9}$$

where m_{PCMS} is the mass of the phase change material, kg; L is the phase change latent heat of the phase change material, kJ/kg.

Tabel 2 The volume and mass of PCMs and rectangular straight fins in the solar collector tube with different number of fins

Fins number	Volume of PCMs /m^3	Mass of PCMs /kg	Volume of fins /m^3	Mass of fins /kg
0	0.00176	3.000	—	—
2	0.00170	2.914	0.0000504	0.402
4	0.00167	2.829	0.0001008	0.804
6	0.00161	2.743	0.0001512	1.207
8	0.00156	2.658	0.0002016	1.609

Fig.8 shows the temperature distribution within the collector tube at the 60th minute. It is evident that the stratification of temperature fields along the radial direction diminishes, and the axial temperature distribution becomes more uniform. This suggests that the uniformity of the temperature distribution in the collector tube correlates positively with the number of fins. The collector tube with 4 fins exhibits the highest temperature distribution, exceeding those with 6 and 8 fins by approximately 10°C.

Fig. 9 displays the heat storage of the collector tube at the 60th minute, with varying numbers of fins. As depicted in fig. 9, as the number of fins increases, the heat storage capacity of the PCMs decreases. Specifically, the total heat storage of the four cases ranging from 1235 to 1269 kJ exhibits negligible variation, which slightly diminishes as the number of fins rises within the range of 2 to 6 fins, while when the number of fins increases from 6 to 8, the total heat storage begins to rise slightly. The total thermal energy storage, governed by both temperature and mass, and when increasing fin number from 6 to 8: the temperature rise from enhanced heat transfer becomes insufficient to offset the heat capacity reduction induced by additional fin mass. Among the four cases, the highest total heat storage is observed with 2 fins which is 1269kJ, followed closely by 4 fins with 1268kJ. Based on the analysis conducted in the first two parts, the composite performance, considering the material temperature, working medium temperature, and heat storage performance, is optimal when there are 4 fins.

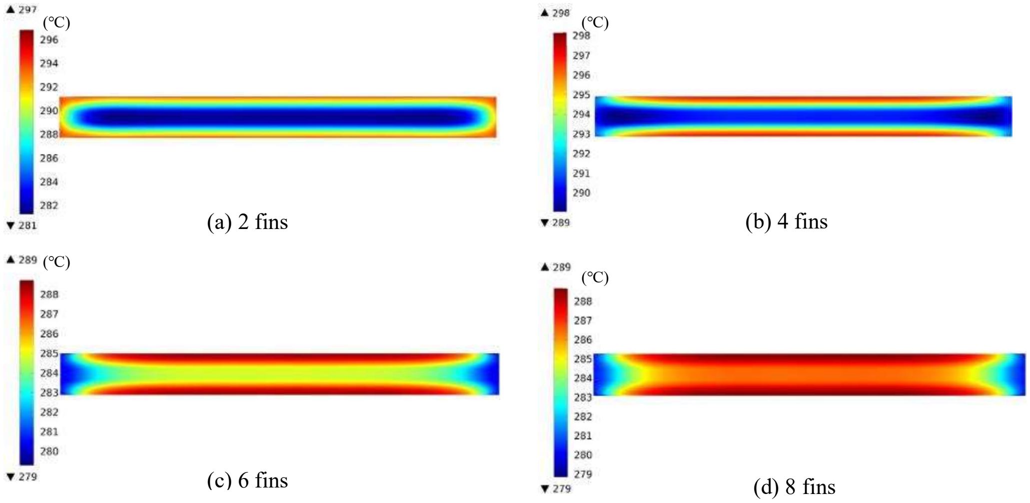

Fig.8 The temperature field distribution of the solar collector tube with different number of rectangular straight fins at the 60th minute

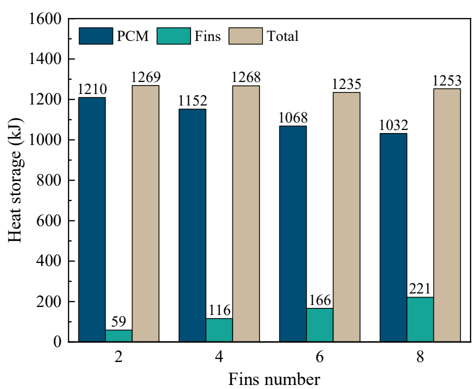

Fig. 9 The heat storage of solar collector tube adding different numbers of fins at the 60th minute

5 Conclusions

The study numerically examines the impact of rectangular straight fins, circular ring fins and trapezoidal ring fins on the thermal properties of solar vacuum collector tubes equipped with an annular PCMs layer. The key findings are as follows: Adding fins decreases the temperature difference between the PCMs and the HTF within the collector tube, thereby enhancing the uniformity of the temperature field distribution within the tube; Among the three fin shapes, rectangular straight fins exhibit the most effective uniformity in radial temperature distribution and have the least adverse impact on the axial temperature field uniformity of the collector tube. However, the phase change process in the collector tube with rectangular straight fins initiates later. When considering collector tubes with 2, 4, 6, and 8 rectangular straight fins, the average temperature of the HTF is lowest with 2 fins and highest with 8 fins. The temperature variation is most stable for tubes with 4 and 6 fins. In terms of heat storage, the collector tube with 2 fins performs best, followed closely by those with 4 fins. Upon comprehensive analysis, the collector tube with 4 fins demonstrates the optimal overall thermal performance. This study was confined to three conventional types of fins. Synergistic integration of fin structures with heat transfer enhancement media (such as nanoparticle) could be expanded in the future research.

Acknowledgment

This work has been carried out with the support of Science and Technology Research Project of Henan Province (232102321088).

References

[1] Gui, Q., et al., Preliminary study on photo-thermal conversion investigation of compound

parabolic concentrator for eliminate light escape in vacuum tube interlayer. *Energy*, 271 (2023), 126979. DOI 10.1016/j.energy.2023.126979

[2] Giacoppo, G., et al., Numerical 3D Model of a Novel Photoelectrolysis Tandem Cell with Solid Electrolyte for Green Hydrogen Production. *Energies*, 16(2023), 4, 1953. DOI 10.3390/en16041953

[3] Ahmed, S. F., et al., Recent progress in solar water heaters and solar collectors: A comprehensive review. *Thermal Science and Engineering Progres*s, 25(2021), 100981. DOI 10.1016/j.tsep.2021.100981

[4] Hua Wang, Shukuan Xie, The effect of annular phase-change material layer on the thermal behavior of solar collector tube. *Journal of energy storage*, 52 (2022), 104948. DOI 10.1016/j.est.2022.104948

[5] Karrar A. Hammoodi, et al., Improving the performance of a pyramid solar still using different wick materials and reflectors in Iraq. *Desalination and Water Treatment*, 285 (2023), pp. 1–10. DOI 10.5004/dwt.2023.29226

[6] S. Shanmugan, et al., A technical appraisal of solar photovoltaic-integrated single slope single basin solar still for simultaneous energy and water generation. *Case Studies in Thermal Engineering*, 54 (2024), 104032. DOI 10.1016/j.csite.2024.104032

[7] Simon, F. et al., Experimental and Numerical Analysis of a PCM-Integrated Roof for Higher Thermal Performance of Buildings, Journal of Thermal Science, 33(2) (2024), pp. 522-536. DOI 10.1007/s11630-023-1909-5

[8] Goel, V., et al., Potential of phase change materials and their effective use in solar thermal applications: A critical review. *Applied Thermal Engineering*, 219 (2023), 119417. DOI 10.1016/j.applthermaleng.2022.119417

[9] Karrar A. Hammoodi, et al., A detailed review of the factors impacting pyramid type solar still performance. Alexandria Engineering Journal, 66(2023), pp.123–154. DOI 10.1016/j.aej.2022.12.006

[10] Karrar A. Hammoodi, et al., Pyramid solar distillers: A comprehensive review of recent techniques. Results in Engineering, 18 (2023), 101157. DOI 10.1016/j.rineng.2023.101157

[11] Sadeghian, A., et al., Effects of rib on cooling performance of photovoltaic modules (PV/PCMs-Rib). *Journal of Central South University*, 28(2021), 11, pp. 3449-3465. DOI 10.1007/s11771-021-4867-7

[12] Huang, M., et al., Phase change material heat storage performance in the solar thermal storage structure employing experimental evaluation. *Journal of Energy Storage*, 46 (2022), 103638. DOI 10.1016/j.est.2021.103638

[13] Balasubramanian, K., et al., Tetrapods based engineering of organic phase change material for thermal energy storage, *Chemical Engineering Journal*, 462 (2023), 141984. DOI10.1016/j.cej.2023.141984

[14] Mebarek-Oudina, F., Chabani, I., Review on nano enhanced PCMs: insight on the PCMs application in thermal management/storage systems. *Energies*, 16 (2023), 3, 1066. DOI10.3390/en16031066

[15] Mebarek-Oudina, F., Chabani, I., Review on Nano-Fluids Applications and Heat Transfer Enhancement Techniques in Different Enclosures. *J. Nanofluids*, 11(2022), pp.155–168. DOI10.1166/jon.2022.1834

[16] Wen, D., Ding, Y., Effective thermal conductivity of aqueous suspensions of carbon nanotubes (carbon nanotube nanofluids). *Journal of thermophysics and heat transfer*, 18(2004), 4, pp. 481-485. DOI 10.2514/1.9934

[17] Saranprabhu MK, Rajan KS., Magnesium oxide nanoparticles dispersed solar salt with improved solid phase thermal conductivity and specific heat for latent heat thermal energy storage. *Renewable Energy*,14(2019), pp.451-9. DOI 10.1016/j.renene.2019.04.027

[18] Bulk, A., et al., Processing Compressed Expanded Natural Graphite for Phase Change Material Composites, *Journal of Thermal Science*, 32(3), 2023, pp. 1213-1226. DOI:10.1007/s11630-022-1578-9

[19] Yao, SG., et al., Evaluation and Optimization of the Thermal Storage Performance of a Triplex-Tube Thermal Energy Storage System with V-Shaped Fins, 32(6), 2023, pp. 2048-2064.

DOI10.1007/s11630-023-1795-x

[20] Abbasov, H. F., The effective thermal conductivity of composite phase change materials with open-cellular metal foams. *International Journal of Thermophysics*, 41(2020), 12, 164. DOI 10.1007/s10765-020-02747-z

[21] Balakrishnan, V. K., et al., Experimental analysis of solar air heater using polygonal ribs in absorber plate integrated with phase change material. *Thermal Science*, 26(2022), 4 Part A, pp. 3187-3199. DOI 10.2298/TSCI210518345V

[22] Yao, Z., Yang, C., Chen, B., Dai, G., & Chen, Y., Computational fluid dynamics analysis of PCMs-based ocean thermal engine with external fin turbulators. *Applied Thermal Engineering*, 238(2024), 122054. DOI10.1016/j.applthermaleng.2023.122054

[23] Li B, et al., Experimental and numerical investigation of a solar collector/storage system with composite phase change materials. *Solar Energy*, 164(2018), pp. 65-76. DOI 10.1016/j.solener.2018.02.031

RECEIVED DATE: 17.02.2025
DATE OF CORRECTED PAPER: 25.03.2025
DATE OF ACCEPTED PAPER: 22.04.2025.